Journal of Physics: Condensed Matter

Short range charge/orbital ordering in $La_{1-x}Sr_xMn_{1-z}B_zO_3$ (B = Cu,Zn) manganites

INSTITUTE OF PHYSICS PUBLISHING JOURNAL OF PHYSICS: CONDENSED MATTER

J. Phys.: Condens. Matter **17** (2005) 351–360 doi:10.1088/0953-8984/17/2/010

Short range charge/orbital ordering in $La_{1-x}Sr_xMn_{1-z}B_zO_3$ (B = Cu, Zn) manganites

Z V Popović[1,2], A Cantarero[1], W H A Thijssen[1,3], N Paunović[2], Z Dohčević-Mitrović[2] and F Sapiña[1]

[1] Materials Science Institute, University of Valencia, PO Box 22085, 46071 Valencia, Spain
[2] Centre for Solid State Physics and New Materials, Institute of Physics, PO Box 68, 11080 Belgrade/Zemun, Serbia

E-mail: zoran.popovic@phy.bg.ac.yu

Received 12 August 2004, in final form 3 December 2004
Published 20 December 2004
Online at stacks.iop.org/JPhysCM/17/351

Abstract

We have measured the reflectivity spectra of $La_{1-x}Sr_xMn_{1-z}B_zO_3$ (B = Cu, Zn; $0.17 \leqslant x \leqslant 0.30$; $0 \leqslant z \leqslant 0.10$) manganites over wide frequency (100–4000 cm^{-1}) and temperature (80–300 K) ranges. Besides the previously observed infrared active modes or mode pairs at about 160 cm^{-1} (external mode), 350 cm^{-1} (bond bending mode) and 590 cm^{-1} (bond stretching mode), we have clearly observed two additional phonon modes at about 645 and 720 cm^{-1} below the temperature T_1 ($T_1 < T_C$), which coincides with the phase transition temperature when the system transforms from ferromagnetic metallic into a ferromagnetic insulator state. This transition is related to the formation of short range charge/orbitally ordered domains. The temperature T_1 of the phase transition is dependent on the doping concentration and for optimally doped samples we have found that $T_1 \approx (0.93 \pm 0.02)T_C$. Electrical resistivity and magnetization measurements versus temperature and magnetic field support the short range charge/orbital ordering scenario.

1. Introduction

During the last decade, $R_{1-x}A_xMnO_3$ pseudocubic manganites (R is a rare-earth metal: La, Pr, Nd, Dy; A is an alkaline earth: Sr, Ca, Ba, Pb) have attracted much attention due to their unique spin-dependent magneto-transport properties. The progress in this field has been recently summarized in [1]. The strong interplay between charge, spin, orbital and lattice degrees of freedom in these materials leads to a variety of phases, such as ferromagnetic metallic (FMM), antiferromagnetic insulator (AFI), ferromagnetic insulator (FMI), cluster glass, spin

[3] Present address: Kamerlingh Onnes Laboratorium, Leiden University, Postbus 9504, 2300 RA Leiden, The Netherlands.

glass and orbitally ordered (OO), antiferromagnetic canted (AFC) and orbitally ordered and charge orbitally ordered (COO). From the technological point of view, the most interesting property of these systems is the colossal magnetoresistance (CMR) [2], which occurs near the Curie temperature T_C, when the oxides undergo a transition from the paramagnetic (PM) to the FM state. The magnetic and transport properties of manganites are believed to be determined by a competition between the superexchange (SE) interaction and the double-exchange (DE) mechanism [3]. Further studies on these materials have shown that other mechanisms influence the phase transitions, among them the electron–phonon interaction arising from the Jahn–Teller (JT) distortion [4], the orbital ordering [5], the electron–electron correlations and the coupling between spin and orbital structure [6].

The orbital degree of freedom is considered to play an important role in manganites [7]. Due to the strong Hund coupling and the crystal field, two e_g orbitals (the $d_{3z^2-r^2}$ and $d_{x^2-y^2}$ orbitals) of the Mn ion are degenerate and one of them is occupied by an electron in the Mn^{3+} ion. In the undoped $LaMnO_3$, the $d_{3x^2-r^2}$ and $d_{3y^2-r^2}$ orbitals are alternately aligned [8]. Whereas a uniform alignment of the d orbitals is experimentally confirmed in lightly and heavily doped manganites [9], experimental evidence of orbital ordering in optimally doped manganites ($\sim$30% Mn^{4+}) has not been reported. Two kinds of mechanisms have been discussed as causes of the orbital ordering. One is due to the SE-type interaction between orbitals in different sites. This interaction originates from the virtual exchange of electrons under the strong on-site electron–electron interactions. A second mechanism is based on the cooperative JT effect, where the lattice distortion occurs cooperatively and lifts the orbital degeneracy in the transition metal ions. The effective interaction between the orbitals in this mechanism is caused by virtual exchange of phonons. Because the on-site Coulomb interaction between electrons was estimated experimentally to be about 7 eV, which is much larger than E_{JT} ($\sim$1 eV) [10], it is believed that the orbital ordering is mainly caused by electronic interactions. Further support for this conclusion can be found in the *ab initio* study of the stability of orbital ordering in $LaMnO_3$, which revealed that OO in both orthorhombic and rhombohedral $LaMnO_3$ has purely electronic origin [11].

The $La_{1-x}Sr_xMnO_3$ system has a very rich structure–property phase diagram, especially for moderately substituted x ($0 \leqslant x \leqslant 0.2$) [12–14]. Three structural phases have been identified at room temperature as a function of the Sr substitutional level for $0 \leqslant x \leqslant 0.2$ [13]. Pure and lightly ($x \leqslant 0.1$) doped $LaMnO_3$ has the orthorhombic $Pbnm$ structure (O′) characterized by large coherent orbital ordering of JT type and $c/a < \sqrt{2}$. The coherent JT distortion decreases with increasing Sr concentration. Above $x \approx 0.1$, a phase (O*) with the same $Pbmn$ orthorhombic symmetry has been observed. This structure is characterized by a considerably smaller coherent JT distortion and $a \approx b \approx c/\sqrt{2}$. In this phase a large incoherent JT distortion has been found. At higher Sr substitutional level, $x \geqslant 0.17$, the rhombohedral $R\bar{3}c$ structure (R), characterized by the absence of a coherent JT orbital ordering, has been reported (all Mn–O bonds have equal length). At low temperatures and low concentrations ($x < 0.1$) the system has an insulating orthorhombic phase O′, which reveals canted antiferromagnetism. For $0.1 \leqslant x \leqslant 0.15$, the ground state is a FMI. For $x \geqslant 0.17$, the ground state is a FMM, revealing an O′ structure for $x < 0.2$ and R structure for $x > 0.2$ [14]. To the best of our knowledge, there is no phase diagram for the Mn site (B site) doped $La_{1-x}Sr_xMnO_3$ system. As regards the B cationic sublattice, great attention has been paid to the B site substitution effect on the charge ordered ground state (i.e., 50% Mn^{4+}) [15], and to the analysis of local magnetic coupling between the magnetic moments of the substituents and Mn ions [16–21]. All substituents have produced a decrease of the transition temperature T_C, which has been attributed to a weakening of the DE interaction due to the structural distortion and the perturbation of the connecting paths for the transport of holes across Mn–O–Mn chains. There are a few results

concerning Mn substitution having the optimum content of Mn^{4+} [22]. The values of T_C for these compounds appear to be clearly related to the mean size of the cations at B sites. In fact, in the case of large Mn substitutional defects, Fadli *et al* [22] have found that the decrease in T_C associated with the increase in z is mainly determined by the local effect of the structural disorder introduced by large substitutional cations, and it is poorly modulated by the magnetic nature of the substitutional metals (Cu^{2+} versus Zn^{2+} and Sc^{3+}) or by the different stoichiometries of the samples (Sc^{3+} versus Cu^{2+} and Zn^{2+}). For a more detailed discussion, see [22].

In this paper we use infrared spectroscopy together with magnetic and transport measurements to study optimally doped $La_{1-x}Sr_xMn_{1-z}B_zO_3$ (B = Cu, Zn; $0.17 \leqslant x \leqslant 0.30$, $0 \leqslant z \leqslant 0.1$) manganites. Previous infrared (IR) spectroscopy measurements on $La_{1-x}Sr_xMnO_3$ samples [23, 24] have revealed that the optical conductivity in the ferromagnetic phase consists of a broad incoherent spectrum accompanied by the strong suppression of a Drude weight [25]. Recently, IR reflectivity measurements on cleaved samples have shown [26] that the Drude-like term is not limited to the very low energy region below 20 meV at low temperatures where the conducting e_g electrons are fully spin polarized. Takenaka *et al* demonstrated that polishing of the sample surface damages the optical spectra of the doped manganites. They concluded that the interpretation based on the *small Drude weight* was wrong, because it appears due to the deterioration of the surface. They also claimed that there are two types of FMM phase below T_C in the $x = 0.17$ single-crystal samples: a 'high temperature incoherent metallic' and a 'low temperature coherent metallic' (Drude) phase.

The origin of the incoherent conductivity in manganites has been discussed by many authors. It has been proposed [26] that JT instability, orbital degrees of freedom and charge ordering can block the coherent motion of the charge carriers. In this paper we have measured infrared reflectivity of optimally doped $La_{1-x}Sr_xMn_{1-z}B_zO_3$ (B = Cu, Zn) samples. With optimum doping we accomplished the minimum vacancies at the A and the B sites, the strongest colossal magnetoresistance effect and we also excluded the possibility of long range charge/orbital ordering. On the other hand, the B site doping offers us the possibility of reducing the concentration of free carriers (the Drude term in the optical conductivity). By comparing the results from optical reflectivity with transport and magnetization measurements we have found that new phonon modes in superposition with an incoherent part in the optical conductivity appear at a temperature $T_1 \approx (0.93 \pm 0.02)T_C$ (for optimum doping). Besides that, the electrical resistivity and the spontaneous magnetization abruptly increase at T_1. These findings are considered as the hallmark of short range charge/orbital ordering.

2. Experiment

Single-phase $La_{1-x}Sr_xMn_{1-z}B_zO_3$ (B = Cu, Zn) samples have been prepared via the acetic acid solution freeze-drying method. This soft procedure makes possible a strict stoichiometric control, and the synthesis variables allow one to maintain a constant proportion of Mn^{4+} (about $32 \pm 2\%$) through the whole series of samples by varying the Sr concentration x. In this way, the concentration of cationic vacancies at A and B sites is kept practically negligible in all cases. The values of x and z in the doping, together with the Curie temperatures (T_C) for all samples investigated, are given in table 1. Room temperature x-ray powder diffraction patterns of the samples used have been completely indexed and refined with rhombohedral perovskite symmetry and the $R\bar{3}c$ space group. Details of the preparation of the samples studied, together with x-ray diffraction and magnetization measurements, have been published elsewhere [22]. Disc shaped pellets were optically polished using diamond paste. The size of the diamond grains was less than 1 μm.

Table 1. Chemical analysis and T_C (in K) for the samples with nominal composition $La_{1-x}Sr_xMn_{1-z}B_zO_{3+\delta}$. The estimated errors in the La/Mn ratios are ∼0.01; the estimated error in the Mn^{4+} content (given in %) is ±1% [22].

z	0.00	0.02	0.04	0.06	0.08	0.10
			B = Cu			
x	0.30	0.274	0.248	0.222	0.196	0.170
Mn^{4+} (%)	31	32	32	32	35	32
δ	0.005	0.010	0.010	0.010	0.023	0.010
T_C	372	358	331	308	274	236
			B = Zn			
x		0.274	0.248	0.222	0.196	0.170
Mn^{4+} (%)		30	31	33	32	33
δ		0	0.005	0.014	0.010	0.014
T_C		350	326	284	233	179

The reflectivity spectra were measured from pellets with a Bomem DA-8 spectrometer. A deuterated triglycine sulfate (DTGS) pyroelectric detector was used to cover the frequency region from 80 to 600 cm^{-1} and a liquid nitrogen cooled Hg–Cd–Te detector was used from 500 to 4000 cm^{-1}. The spectra were collected with 2 cm^{-1} resolution, by averaging 1000 interferograms per spectrum. For the low temperature measurements a Janis Super Tran continuous flow cryostat (ST-100) was used. Magnetization data were taken in a superconducting quantum interference device (SQUID) magnetometer with a 50 kOe magnet in the 5–300 K temperature range. The magnetoresistivity measurements were performed in a Cryogenic Ltd liquid helium free superconducting magnet by the van der Pauw method between 2 and 300 K with applied magnetic fields up to 14 T.

3. Results and discussion

Figure 1(a) shows the room temperature reflectivity spectra of $La_{1-x}Sr_xMn_{1-z}Cu_zO_3$ ($0 \leqslant z \leqslant 0.08$) polycrystalline samples in the spectral range from 500 to 900 cm^{-1}. The reflectivity spectra of the $La_{0.83}Sr_{0.17}Mn_{0.9}Cu_{0.1}O_3$ sample at different temperatures are given in figure 1(b). The Curie temperature T_C of each sample is defined as the temperature corresponding to the minimum of dM/dT, where the magnetization $M(T)$ was measured at a magnetic field of 1 T [22]. Far infrared reflectivity spectra of the $z = 0.1$ sample at different temperatures are shown in figure 2. As we have discussed in [27], these spectra consist of two mode doublets with TO frequencies at about 144/166 and 340/375 cm^{-1} and a single mode at about 590 cm^{-1}. The doublets can be assigned as the rhombohedral symmetry A_u/E_u mode pairs. The lowest frequency doublet originates from the vibrations of the La ions against the MnO_6 octahedra along the z- and $y(x)$-axes, respectively. The next doublet of A_u^2 and E_u^2 modes represents bond bending O–Mn–O vibrations, while the A_u^3/E_u^3 mode doublet appears as a degenerate mode in the infrared spectra at room temperature, which is in agreement with lattice dynamical calculations [28]. For more details on phonon properties of B site doped manganites, see [27]. The most intriguing features in figures 1 and 2 are two additional modes, which appear at about 645 and 720 cm^{-1}. These modes show up together with an incoherent part in the optical conductivity in the ferromagnetic phase only. It is worth noting that the room temperature infrared spectra for $0 \leqslant z \leqslant 0.08$ samples, figure 1(a), resemble the $z = 0.1$ spectra at temperatures lower than 220 K, figure 1(b). In order to clarify these findings we

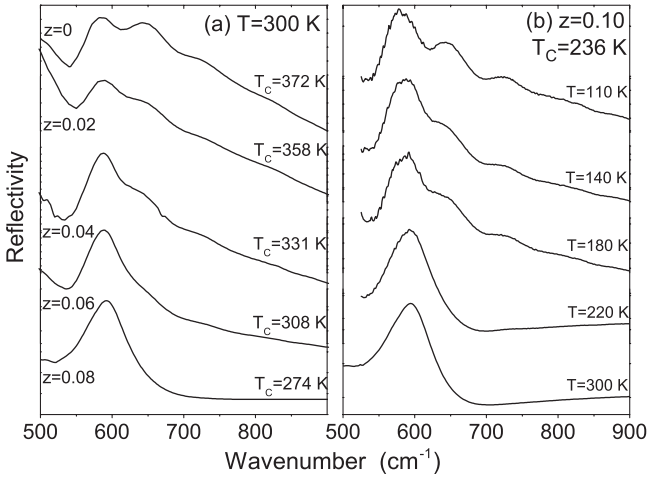

Figure 1. (a) Room temperature infrared reflectivity spectra of the $La_{1-x}Sr_xMn_{1-z}Cu_zO_3$ ($0 \leqslant z \leqslant 0.08$) samples in the 500–900 cm^{-1} spectral range; T_C denotes the Curie temperature. (b) Infrared reflectivity spectra of the $La_{0.83}Sr_{0.17}Mn_{0.9}Cu_{0.1}O_3$ sample at different temperatures in the same spectral range.

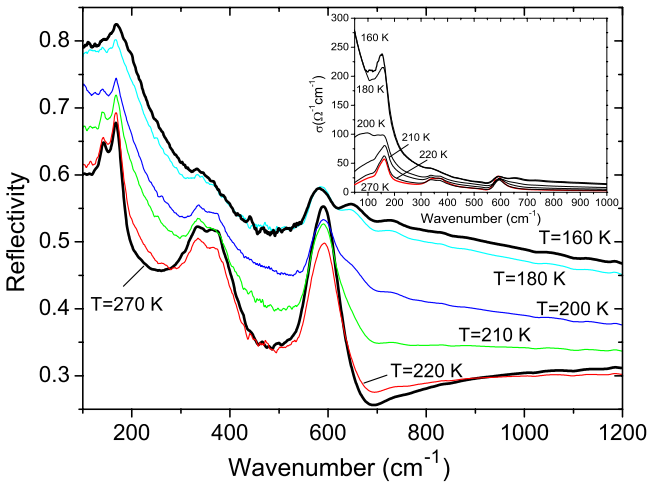

Figure 2. Far infrared reflectivity spectra of the $La_{0.83}Sr_{0.17}Mn_{0.9}Cu_{0.1}O_3$ sample at different temperatures. Inset: optical conductivity calculated from the reflectivity spectra using a Kramers–Kronig analysis.

(This figure is in colour only in the electronic version)

have measured the temperature dependence of the magnetization and the electrical resistivity (figure 3), and the magnetic field dependence of the magnetization (figure 4) and the electrical resistivity as a function of the magnetic field (figure 5) in the same sample.

Figure 3 shows the magnetization curves for the $La_{0.83}Sr_{0.17}Mn_{0.9}Cu_{0.1}O_3$ sample measured under an applied magnetic field of 1 Oe, together with the electrical resistivity versus temperature spectrum of the same sample. Several temperature-dependent transitions are clearly observed in figure 3. The upper transition denoted as T_s (253 K) appears as a hysteresis loop corresponding to the structural phase transformation from the rhombohedral (R) to the

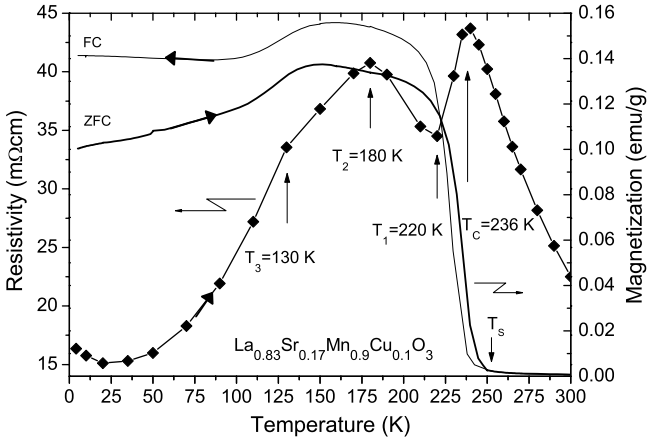

Figure 3. The temperature dependence of the specific electric resistivity and the spontaneous magnetization of the $La_{0.83}Sr_{0.17}Mn_{0.9}Cu_{0.1}O_3$ sample. The magnetization was measured at $H = 1$ Oe in zero-field cooling (ZFC) and field cooling (FC) processes.

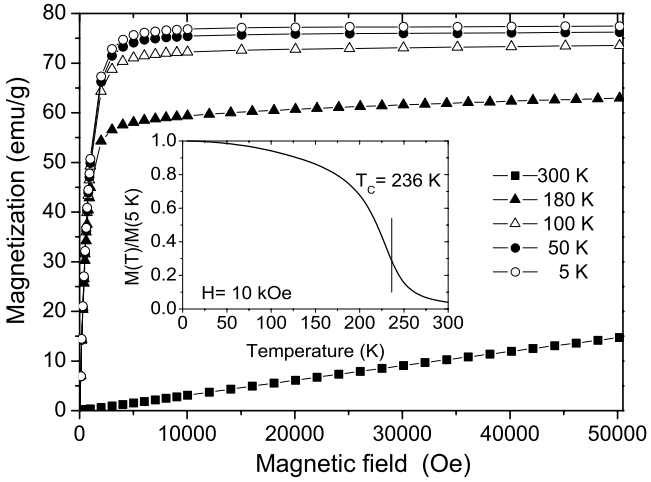

Figure 4. Magnetization versus magnetic field dependence at different temperatures for the $La_{0.83}Sr_{0.17}Mn_{0.90}Cu_{0.10}O_3$ sample. Inset: normalized magnetization $[M(T)/M(5\text{ K})]$ versus temperature for the same sample at $H = 10$ kOe.

orthorhombic (O*) phase. This phase transition, which appears as an increase of resistivity with cooling, has been observed in the single crystals [29] and ceramic samples [13] with the same composition. T_s shifts abruptly to lower temperatures with increasing Sr substitution. The second transition at lower temperatures ($T_C = 236$ K) is the PM to FM phase transition. The Curie temperature T_C corresponds to the maximum slope in the $M(T)$ curve and coincides with the local maximum of resistivity. Below T_C, in the ferromagnetic phase, the resistivity decreases rapidly with decreasing temperature between T_C and T_1. At T_1 (220 K) an abrupt increase of resistivity is observed. Below this temperature an additional increase of the spontaneous magnetization (figure 3) and the appearance of new phonon modes (figure 2) are observed.

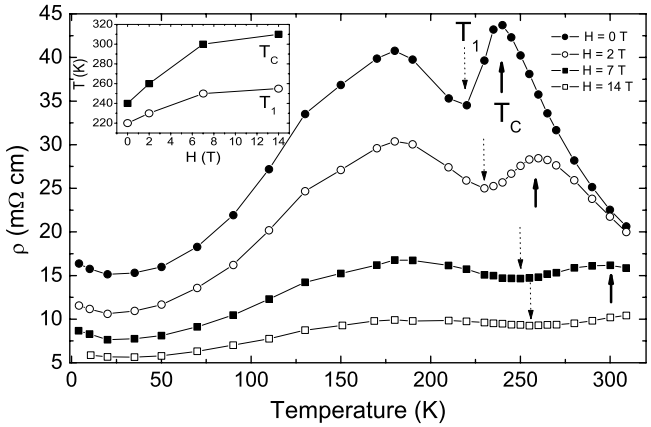

Figure 5. The temperature dependence of the specific electric resistivity of the $La_{0.83}Sr_{0.17}Mn_{0.9}Cu_{0.1}O_3$ sample at different magnetic fields. Inset: the field dependence of T_C and T_1.

Figure 4 shows the field dependence of the magnetization $M(H)$ for $La_{0.83}Sr_{0.17}Mn_{0.9}Cu_{0.1}O_3$ at different temperatures. Saturation of magnetization at a low field (∼0.5 T) is an indication of ferromagnetic order for all measurement temperatures except room temperature, since the sample is in the paramagnetic state. According to figures 3 and 4 we conclude that the phase below T_1 is also ferromagnetic but insulating ($d\varrho/dT < 0$ for $T_2 < T < T_1$). Several microscopic origins have been proposed to explain the resistivity rise below T_C, among them a long range polaron (charge) ordering [30], a long range orbital ordering [31] and a long range antiferromagnetic order [32]. Recently, it has been shown that the insulating ground state in manganites does not require the development of long range charge or orbital order. The resistivity upturn was associated with a diffuse structural transition characterized by the strong reduction of the orthorhombicity [33], a remarkable rotation of the easy magnetization axis [34], or the formation of an orbitally ordered domain state [35]. Here, the B site doping destroys the coherence of the long range orbital and/or charge alternation. On the other hand, local lattice distortion created by B site substitution is accompanied with localization of e_g holes (polarons) and their short range correlations. The short range polaron–polaron correlations can also be regarded as short range charge ordering, which, as discussed in [36], drives the orbital ordering. The insulating behaviour below T_1 can be understand in terms of competition between the short range orbital/charge order and the long range FM order.

The so-called 'phase separation' concept [1] has also been used to explain this phase transition. In the present case, two types of ferromagnetic phase exist: one is metallic (FMM) and the second one insulating (FMI). The FMM state is gradually destroyed by B site substitution, and the magnetic spontaneous state is driven into a cluster state, which explains the relative large disagreement between zero-field cooled (ZFC) and field cooled (FC) thermomagnetization curves (figure 3). On lowering the temperature, FM clusters grow up and an insulator/metal transition at about 180 K can be explained by percolative transport through ferromagnetic metallic domains [37].

As was argued in the case of $La_{0.88}Sr_{0.12}MnO_3$ [31], the ferromagnetic insulator phase is driven by SE interaction caused by type II orbital ordering (the hybridization of $d_{z^2-x^2}$ ($d_{y^2-z^2}$) and $d_{3x^2-r^2}$ ($d_{3y^2-r^2}$) orbitals). The additional increase of magnetization at T_1 appears due to the abrupt variation of the magnetic exchange interaction energies (SE versus DE crossover) [31]. The transition from the FMM state into a FMI one at T_1 is also followed by a structural

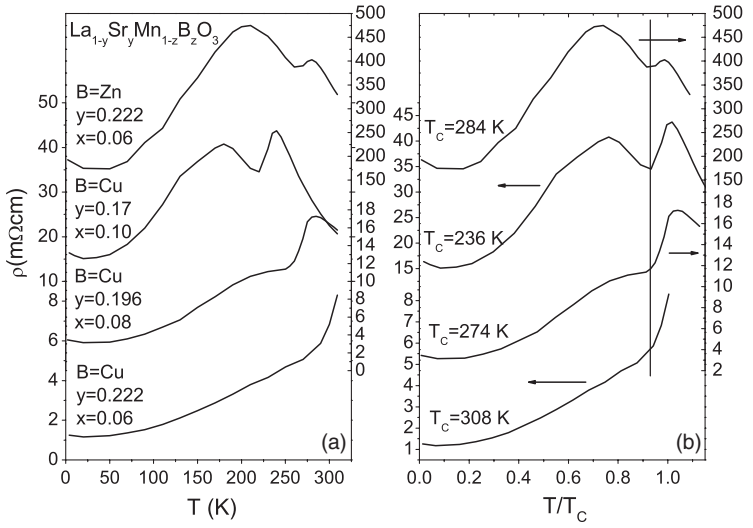

Figure 6. (a) The temperature dependence of the electrical resistivity of the $La_{1-x}Sr_xMn_{1-z}Cu(Zn)_zO_3$ samples. (b) The same results represented on a temperature scale normalized to T_C. The solid vertical line denotes the value $T_1/T_C = 0.93$.

change from orthorhombic O* to the pseudocubic O** phase [31]. The crystal structure of the O** phase has been described as orthorhombic [31], pseudocubic [14] or triclinic [38]. New infrared (IR) phonons at about 645 and 720 cm^{-1} appear in this phase. We assigned them as antistretching and breathing infrared active modes at the R point of $Pm3m$ cubic symmetry. The calculated frequencies [28] of these modes are 646 and 716 cm^{-1}, very close to our experimental findings. Appearance of zone edge phonons derived from the cubic structure of $LaMnO_3$ can be looked at as a consequence of doubling the unit cell in the O** phase. These zone edge phonons become IR active simply through a zone folding effect. On the other hand, the zone edge phonons are coupled with the spin wave energies, as has been recently shown by Moussa *et al* [39] for the FI phase in $La_{0.875}Sr_{0.125}MnO_3$, suggesting a complex ground state for the FI phase with mixed magnetic and phononic excitations.

Figure 5 shows the temperature dependence of the electrical resistivity of the $La_{0.83}Sr_{0.17}Mn_{0.9}Cu_{0.1}O_3$ sample at different magnetic fields. The field dependence of T_C and T_1 is given in the inset of figure 5. As is shown in the inset, both T_C and T_1 increase with applied magnetic field. It is known that the DE interaction increases with increasing magnetic field; this is followed by an increase of conductivity and T_C. Also an increase of T_1 with magnetic field has been theoretically predicted [10] and experimentally established [31]. All these facts are in complete agreement with our findings (figure 5).

Figure 6 presents the temperature dependence of the electrical resistivity for several B site optimally doped samples. As is shown in figure 6(a), the increase of B site doping generally leads to an increase of the electrical resistivity of the samples and the appearance of a 'double-peak' structure in the electrical resistivity versus temperature graphs. The increase of the electrical resistivity originates from the hole scattering by the random potential of the B site impurities. On the other hand, a decrease of T_C is a consequence of the weakening of the DE due to the crystal distortion caused by the B site doping and/or the perturbation of the connecting paths for the transport of holes across Mn–O–Mn, that substantially prevents the DE interaction. In figure 6(b) we show the same spectra as in figure 6(a) but on a temperature

scale normalized to T_C. The main conclusion which can be drawn from figure 6 is that the temperature T_1 appears always at almost the same position relative to T_C, regardless the B site dopant ions. That means that *the interplay of the short range correlations and ferromagnetic DE interaction can lead to a charge/orbitally ordered domain state below* T_1. The transition temperature T_1 depends on the doping level. Since we kept the doping level in all samples nearly constant (∼32%), the ratio T_1/T_C remains unchanged. We found here that for optimum doping $T_1/T_C \approx 0.93 \pm 0.02$. For a different doping level the T_1/T_C ratio has a different value (for example, $T_1/T_C \approx 0.85$ in the case of $x = 0.12$ [31]).

Let us go back to figure 3, where the resistivity versus temperature data are shown. The resistivity of the $La_{0.83}Sr_{0.17}Mn_{0.9}Cu_{0.1}O_3$ sample increases when the temperature decreases below T_1. At $T_2 = 180$ K a sharp decrease in the resistivity is observed, indicating a new phase transition. We believe that for temperatures below 180 K the magnetic structure becomes fully aligned (canted ferromagnetic), as has been found in $LaMnO_{3.15}$ samples with the same doping level (30% of Mn^{4+}) [40] and in $x = 0.175$ samples with rhombohedral symmetry [41]. A better spin alignment results in an improved DE electron transfer which in turn enhances the spin ordering. Thus, the phase transition is manifested through an additional increase of the spontaneous magnetization at about 180 K (see the ZFC curve in figure 3), an insulator–metal transition (the system becomes metallic below T_2) and a crossover from the incoherent to a coherent part (Drude) in the optical conductivity (see the inset in figure 2).

Finally, we have found that the structural transition at about $T_3 \approx 130$ K, already found in the $x = 0.17$ samples [13], also leaves a fingerprint in the resistivity (saddle point) and the spontaneous magnetization (slope change) spectra of our sample in figure 3.

In conclusion, we present optical and magneto-transport measurements of B site doped $La_{1-x}Sr_xMn_{1-z}B_zO_3$ manganites. The doping level was kept constant at ∼32 %. An abrupt increase in both the electrical resistivity and the spontaneous magnetization, the appearance of new phonon modes in superposition with an incoherent part in the optical conductivity and increase of T_1 on increase of the magnetic field are considered as the hallmarks of short range charge/orbital rearrangements that take place on cooling. Our results strongly suggest that the competition between short range correlations and ferromagnetic DE interaction in $La_{1-x}Sr_xMn_{1-z}B_zO_3$ manganite samples can lead to a phase transition from a FMM orbitally disordered to a FMI charge/orbitally ordered domain state, which appears at about $T_1 \approx (0.93 \pm 0.02)T_C$ for optimum doping.

Acknowledgments

We thank José-María Martínez-Agudo for the magnetic measurements. One of us (ZVP) thanks the Ministry of Education, Culture and Sport of Spain for financial support. This work was supported by the EU through a TMR grant (HPRN-CT2000-00021) and the Serbian MST under the project No 1469.

References

[1] Dagotto E 2003 Nanoscale phase separation and colossal magnetoresistance *The Physics of Manganites and Related Compounds* (*Springer Series in Solid-State Sciences* vol 136) (Berlin: Springer)
[2] von Helmolt R, Wecker J, Holzapfel B, Schultz L and Samwer K 1993 *Phys. Rev. Lett.* **71** 2331
[3] Zener Z 1951 *Phys. Rev.* **82** 403
[4] Millis A J, Littlewood P B and Shraiman B I 1995 *Phys. Rev. Lett.* **74** 5144
[5] Maezono R, Ishihara S and Nagaosa N 1998 *Phys. Rev.* B **57** R13993
[6] Ishihara S, Inoue J and Maekawa S 1997 *Phys. Rev.* B **55** 8280
[7] van den Brink J, Khaliullin G and Khomskii D 2002 *Preprint* cond-mat/0206053

[8] Goodenough J B 1955 *Phys. Rev.* **100** 564
[9] Okamoto S, Ishihara S and Maekawa S 2000 *Phys. Rev.* B **61** 14647
[10] Okamoto S, Ishihara S and Maekawa S 2002 *Phys. Rev.* B **65** 144403
[11] Medvedeva J E, Korotin M A, Anisimov V I and Freeman J 2002 *Phys. Rev.* B **65** 172413
[12] Urushibara A, Moritomo Y, Arima T, Asimitsu A, Kido G and Tokura Y 1995 *Phys. Rev.* B **51** 14103
[13] Dabrowski B, Xiong X, Bukowski Z, Dybzinski R, Klamut P W, Siewenie J E, Chmaissem O, Shaffer J, Kimball C W, Jorgensen J D and Short S 1999 *Phys. Rev.* B **60** 7006
[14] Paraskevopoulos M, Mayr F, Hemberger J, Loidl A, Heichele R, Maurer D, Müller V, Mukhin A A and Balbashov A M 2000 *J. Phys.: Condens. Matter* **12** 3993
[15] Maignan A, Caignert V, Simon Ch, Hervieu M and Raveau B 1995 *J. Mater. Chem.* **5** 1091
Mahesh R, Mahendrian R, Raychaudhuri A K and Rao C N R 1995 *J. Solid State Chem.* **120** 204
[16] von Helmolt R, Haupt L, Bärner K and Sondermann U 1992 *Solid State Commun.* **82** 693
[17] Yuan C L, Zhu Y and Ong P P 2001 *Solid State Commun.* **120** 495
[18] Lakshmi L S, Sridharan V, Natarajan D V, Chandra S, Sastry V S, Radhakrishnan T S, Pandian P, Joseyphus R J and Narayanasamy A 2002 *J. Magn. Magn. Mater.* **257** 195
[19] Zheng L, Xu X, Pi L and Zhang Y 2000 *Phys. Rev.* B **62** 1193
[20] Yusuf S M, Sahana M, Dörr K, Rößler U K and Müller K H 2002 *Phys. Rev.* B **66** 064414
[21] Huang Y H, Liao C S, Wang Z M, Li X H and Yan C H 2002 *Phys. Rev.* B **65** 184423
[22] El-Fadli Z, Redouane Metni M, Sapiña F, Martínez E, Folgado J V and Beltrán A 2002 *Chem. Mater.* **14** 688 (tables of refined structural parameters for the rhombohedral setting are available free of charge at http://pubs.acs.org)
[23] Okimoto Y, Katsufuji T, Ishikawa T, Arima T and Tokura Y 1997 *Phys. Rev.* B **55** 4206
[24] Okimoto Y, Katsufuji T, Ishikawa T, Urushibara A, Arima T and Tokura Y 1995 *Phys. Rev. Lett.* **75** 109
[25] Saitoh E, Asimitsu A, Okimoto Y and Tokura Y 2000 *J. Phys. Soc. Japan* **69** 3614
[26] Takenaka K, Iida K, Sawaki Y, Sugai S, Morimoto Y and Nakamura A 1999 *J. Phys. Soc. Japan* **68** 1828
Takenaka K, Sawaki Y and Sugai S 1999 *Phys. Rev.* B **60** 13011
[27] De Marzi G, Popović Z V, Cantarero A, Dohčević-Mitrović Z, Paunović N, Bok J and Sapiña F 2003 *Phys. Rev.* B **68** 064302
[28] Abrashev M V, Litvinchuk A P, Iliev M N, Meng R L, Popov V N, Ivanov V G, Chakalov R A and Thomsen C 1999 *Phys. Rev.* B **59** 4146
[29] Asamitsu A, Moritomo Y, Tomioka Y, Arima T and Tokura Y 1995 *Nature* **373** 407
[30] Yamada Y, Hino O, Nohdo S and Kanao R 1996 *Phys. Rev. Lett.* **77** 904
[31] Nojiri H, Kaneko K, Motokawa M, Hirota K, Endoh Y and Takahashi K 1999 *Phys. Rev.* B **60** 4142
[32] Kawano H, Kajimoto R, Kubota M and Yoshizawa H 1996 *Phys. Rev.* B **53** R14709
[33] Biotteau G, Hennion M, Moussa F, Rodríguez-Carvajal J, Pinsard L, Revcolevschi A, Mukovskii Y M and Shulyatev D 2001 *Phys. Rev.* B **64** 104421
[34] Markovich V, Fita I, Puzniak R, Tsindlekht M I, Wisniewski A and Gorodetsky G 2002 *Phys. Rev.* B **66** 094409
[35] Papavassiliou G, Pissas M, Belesi M, Fardis F, Dolinsek J, Dimitropoulos C and Ansermet J P 2003 *Phys. Rev. Lett.* **91** 147205
[36] Zimmermann M v, Hill J P, Gibbs D, Blume M, Casa D, Keimer B, Murakami Y, Tomioka Y and Tokura Y 1999 *Phys. Rev. Lett.* **83** 4872
[37] Uehara M, Mori S, Chen C H and Cheong S W 1999 *Nature* **399** 560
[38] Tsuda K, Tanaka M, Hirota K and Endoh Y 2001 *J. Phys. Soc. Japan* **70** 1010
[39] Moussa F, Hennion M, Kober P, Wang F, Carvajal-Rodríguez J, Reutler P, Mukovski Y M and Shulyatev D 2003 *J. Magn. Magn. Mater.* **258/259** 259
Moussa F, Hennion M, Wang F, Kober P, Rodríguez-Carvajal J, Reutler P, Pinsard L and Revcolevschi A 2003 *Phys. Rev.* B **67** 214430
[40] Alonso J A, Martínez-Lope M J, Casáis M T and Muñoz A 1997 *Solid State Commun.* **102** 7
[41] Xiong X, Dabrowski B, Chmaissem O, Bukowski Z, Kolesnik S, Dybzinski R, Kimball C W and Jorgensen J D 1999 *Phys. Rev.* B **60** 10186